# Electrical Manipulation of Spins in the Rashba Two Dimensional Electron Gas Systems



doi: 10.1063/1.3117232

# Electrical manipulation of spins in the Rashba two dimensional electron gas systems

Junsaku Nitta,[1,2,3,a)] Tobias Bergsten,[2,3,4] Yoji Kunihashi,[1] and Makoto Kohda[1,2]
[1]*Graduate School of Engineering, Tohoku University, 6-6-02 Aramaki-Aza Aoba, Aoba-ku, Sendai 980-8579, Japan*
[2]*CREST-JST, Sanban-cho 15, Chiyoda-ku, Tokyo 102-0075, Japan*
[3]*NTT Basic Research Laboratories, 3-1 Morinosato-Wakamiya, Atsugi-shi 243-0198, Japan*
[4]*Cavendish Laboratory, Cambridge University, J. J. Thomson Avenue, CB3 0HE Cambridge, United Kingdom*

(Received 18 August 2008; accepted 17 March 2009; published online 18 June 2009)

We present our theoretical and experimental studies on manipulation of electron spins based on the Rashba spin-orbit interaction (SOI) in semiconductor heterostructures. Quantum well (QW) thickness dependence of the Rashba SOI strength $\alpha$ is investigated in InP/InGaAs/InAlAs asymmetric QWs by analyzing weak antilocalization. Two different QW thicknesses show inverse $N_s$ dependence of $|\alpha|$ in the same heterostructures. This inverse $N_s$ dependence of $|\alpha|$ is explained by the $\boldsymbol{k}\cdot\boldsymbol{p}$ perturbation theory. We confirm that narrow wires are effective to suppress the spin relaxation. Spin interference effects due to spin precession are experimentally studied in small array of mesoscopic InGaAs rings. This is an experimental demonstration of a time reversal Aharonov–Casher effect, which shows that the spin precession angle in an InGaAs channel can be controlled by an electrostatic gate. © *2009 American Institute of Physics*. [DOI: 10.1063/1.3117232]

## I. INTRODUCTION

Spin degree of freedom is so far mainly manipulated by an external magnetic field. Most important experiment of spin manipulation was performed by Stern and Gerlach.[1] By using inhomogeneous magnetic fields, they discovered the spatial separation of spin-up and down. Thanks to this discovery, the concept of spin 1/2 was established. Another important experiment was a neutron spin 1/2 interferometer.[2,3] It was experimentally confirmed that a $4\pi$ rotation of spin is necessary to return to the spin original state. This is another triumph of quantum mechanics. The purpose of this paper is to demonstrate that *electrical* manipulation of spins can be possible in mesoscopic semiconductor systems by using the Rashba spin-orbit interaction (SOI).[4] The electrical manipulation of spins opens up a new field of spintronics.

Spintronics is the art of controlling the spin degree of freedom of electrons and their movement in order to perform specific operations.[5–8] It is known that an inversion asymmetry lifts the spin degeneracy. The Rashba SOI caused by a structural inversion asymmetry (SIA) is of importance for spintronics since the strength of SOI can be controlled by applying a gate voltage on top of a two dimensional electron gas (2DEG).[9–11] The SOI gives rise to a momentum-dependent effective magnetic field, which can be used for manipulation of spins. The Datta–Das spin field effect transistor (FET) (Ref. 12) requires gate controlled spin orientation in the 2DEG channel. Many interesting spintronics devices are based on the gate controlled Rashba SOI. We have proposed a mesoscopic Stern–Gerlach spin filter[13] by a spatial distribution of the Rashba SOI strength. In this Stern–Gerlach spin filter, we can expect spin polarized carriers in nonmagnetic semiconductor 2DEGs without using an external magnetic field. In contrast to the spin Hall effects,[14–19] the spin polarized carriers in narrow channels are conserved quantity in the presence of SOI, and high spin polarization can be expected by adjusting proper parameters. On the other hand, a momentum-dependent effective magnetic field due to the SOI randomizes spin orientations after scattering events. A key ingredient for spintronics is to suppress the spin relaxation while keeping the strength of SOI since the SOI plays a double-edged sword for spin manipulation and spin relaxation. It is shown that spin relaxation is suppressed in narrow wires.[20,21] We have confirmed that narrow wires are effective to suppress the spin relaxation.

An electron acquires a phase around magnetic flux due to the vector potential, leading to the Aharonov–Bohm (AB) effect in an interference loop. From the view point of inherent symmetries between magnetic field and electric field in the Maxwell equations, Aharonov and Casher[22] predicted that a magnetic moment acquires a phase around a charge flux line. It should be noted that the original Aharonov–Casher (AC) effect was proposed for charge neutral particle since the electric field modifies the trajectory of charged particle in the same sense as the original AB effect was predicted in the situation where magnetic flux should not exist in an electron path. Cimmino *et al.*[23] managed to perform the AC interference experiment in a neutron (having spin 1/2 but no charge) beam loop using a voltage of 45 kV to create the electric field. However, modified precession angle of neutron spin was only 2.2 mrad since the SOI is very weak in vacuum. Mathur and Stone[24] proposed the electronic AC effect in a mesoscopic interference loop made of GaAs 2DEG with the Dresselhaus[25] SOI. We have proposed a spin interference device based on the Rashba SOI (Ref. 41) and con-

[a)]Author to whom correspondence should be addressed. Electronic mail: nitta@material.tohoku.ac.jp.

 

firmed the gate electric field controlled spin interference.[27] This is an experimental demonstration of AC effect.

In this paper, we discuss the enhancement in SOI in semiconductor heterostructures and the origin of Rashba SOI in Sec. II. In Sec. III, we present our experimental results on quantum well (QW) thickness dependence of gate controlled SOI and suppression of spin relaxation in narrow wires. An operational principle of spin interferometer utilizing the Rashba SOI is discussed in Sec. IV. The conductance of the spin interferometer shows an oscillatory behavior as a function of the Rashba SOI. This is very similar to the Datta–Das spin FET (Ref. 12) in which ferromagnetic source and drain electrodes are necessary. In contrast, the spin interference device works without ferromagnetic electrodes. In Sec. V, we review an experimental demonstration of the spin interference using small arrays of mesoscopic InGaAs 2DEG rings. This spin interference is the AC effect of time reversal symmetric paths and is the electromagnetic dual to the Al'tshuler–Aronov–Spivak (AAS) effect.[28] We demonstrate that we can control the spin precession angle with an electrostatic gate and modulate the interference pattern over several periods.[27] The reason for the clear observation of AC effect is that the SOI effect is much enhanced in semiconductor heterostructures in comparison with that in the vacuum. The gate controlled spin precession angle and suppression of spin relaxation in narrow wires are crucial for spintronics applications.

## II. ORIGIN OF RASHBA SOI

Not only an external magnetic field but also an electric field lifts spin degeneracy when SOI plays a role. The SOI is a relativistic effect on a particle with spin, which is moving with a velocity $\vec{v}$ through an electric field $\vec{E}$. In the particle's frame of reference, $\vec{E}$ is Lorentz transformed into the magnetic field $\vec{B}$, which is perpendicular to the electric field and to the direction of movement,

$$\vec{B} = -\frac{\vec{v}\times\vec{E}}{c^2} = -\frac{\vec{p}\times\vec{E}}{m_0 c^2}. \tag{1}$$

Here $c$ is the light velocity, $m_0$ is mass of electron, and $\vec{v}$ is an electron velocity. In analogy to the Zeeman effect, the SOI is given by an inner product of magnetic moment and magnetic field and is written as

$$H_{\mathrm{SO}} = -\mu_B \vec{\sigma}\cdot\left(\frac{\vec{p}\times\vec{E}}{2m_0 c^2}\right). \tag{2}$$

Here $\mu_B$ and $\vec{\sigma}$ are the Bohr magneton and the Pauli spin matrix, respectively. A factor 1/2 difference stems from the relativistic effect. The SOI effect is small and negligible for nonrelativistic momentum $p=\hbar k \ll m_0 c$. However, it is drastically enhanced in semiconductors with energy gap $E_g$. The Dirac gap $E_D=2m_0c^2\approx 1$ MeV in the denominator of Eq. (2) is replaced by the energy gap $E_g \approx 1$ eV according to the $\boldsymbol{k}\cdot\boldsymbol{p}$ perturbation theory.[11,29] In solids, wave functions of electrons are described by a product of an envelope function and a Bloch function. The enhancement in SOI is due to the contribution from a quickly oscillating Bloch function, which has large momentum and feels a strong electric field near atomic cores.[29] This enhancement in SOI is of critical importance for electrical manipulation of spins.

The confinement of electrons in a 2DEG is generally due to a QW. Band offsets of the boundary materials or applied voltages lead to an asymmetry of the QW. The breaking of spatial inversion symmetry results in the lift in spin degeneracy. This is the so-called Rashba SOI.[4] The asymmetry of the QW yields a macroscopic electric field. To have a finite spin splitting, we need both a macroscopic electric field and a microscopic electric field from the atomic core. The SIA spin splitting energy is proportional to the macroscopic electric field times a prefactor that depends on the matrix element of the microscopic SOI.

It should be noted that the Dresselhaus[25] SOI is independent of any macroscopic electric fields. The Rashba Hamiltonian for a 2DEG in an asymmetric QW is given by

$$H_R = \frac{\alpha}{\hbar}(\vec{p}\times\vec{\sigma})\cdot\hat{z} = \alpha(k_x\sigma_y - k_y\sigma_x). \tag{3}$$

Here $\hat{x}$ and $\hat{y}$ axes are in the 2DEG plane, and $\alpha$ is the Rashba SOI parameter. The spin splitting energy at the Fermi energy is given by $\Delta_R=2\alpha k_F$, where $k_F$ is the Fermi momentum. According to the $\boldsymbol{k}\cdot\boldsymbol{p}$ perturbation theory,[11,29] the Rashba SOI parameter $\alpha$ is given by the following equation:

$$\alpha = \frac{\hbar^2 E_p}{6m_0}\langle\Psi(z)|\frac{d}{dz}\left(\frac{1}{E_F - E_{\Gamma_7}(z)} - \frac{1}{E_F - E_{\Gamma_8}(z)}\right)|\Psi(z)\rangle, \tag{4}$$

where $\Psi(z)$ is the wave function for the confined electron, $E_p$ is the interband matrix element, $E_F$ is the Fermi energy in the conduction band, and $E_{\Gamma_7}(z)$ and $E_{\Gamma_8}(z)$ are positions of the band edge energies for $\Gamma_7$ (spin split off band) and $\Gamma_8$ (the highest valence band) bands, respectively. Contribution to Eq. (4) can be split into two parts: (i) the field part, which is related the electric field in the QW, and (ii) interface part, which is related to band discontinuities at the heterointerface.

For many years, there has been an intense discussion about the Rashba SOI. It was thought that the Rashba SOI should be very small because the average electric field for the bound state is zero, i.e., $\langle E\rangle=0$, in order to satisfy the condition that there is no force acting on a bound state. In fact this controversy is resolved by Eq. (4). It is clear that the Rashba spin splitting in the conduction band originates from the electric field in the valence band.[11,29] Equation (4) also shows that the strength of Rashba SOI can be controlled by the gate electric field on top of the 2DEG.[9–11]

## III. GATE CONTROLLED RASHBA SOI AND SUPPRESSION OF SPIN RELAXATION IN NARROW WIRES

By applying the gate bias voltage in semiconductor heterostructures, not only potential gradient but also the electron wave function confined in the heterostructures is modulated. In Eq. (4), the strength of the Rashba SOI is determined not only internal electric field but also electron probability density $|\Psi(z)|^2$. It implies that QW thickness, which determines the confinement of the wave function, affects the overall

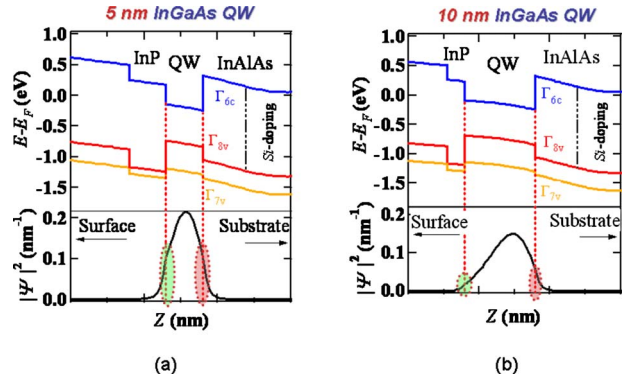


FIG. 1. (Color online) The calculated band structure and electron probability density of InP/InGaAs/InAlAs asymmetric QW with (a) 5 and (b) 10 nm QWs. $\Gamma_6$, $\Gamma_7$, and $\Gamma_8$ are conduction band, heavy hall band, and spin split off band, respectively.

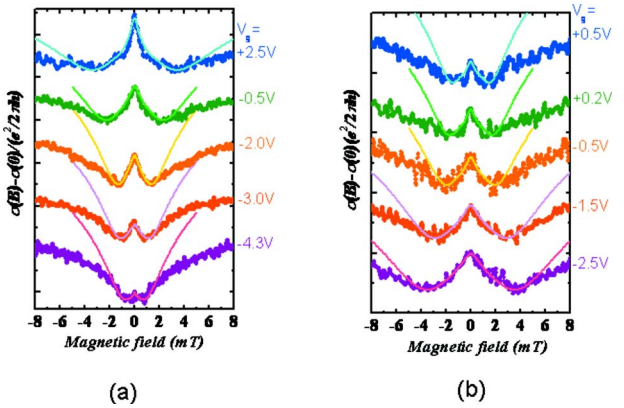


FIG. 2. (Color online) Results of magnetoconductance measurement for (a) 5 and (b) 10 nm QWs with various gate bias voltages at $T=3.8$ K. Unit of vertical axis is $e^2/2\pi h$. Thick curves are experimental data, and solid lines are fitted data by the Golub model.

strength of the Rashba SOI. Thus, we studied the QW thickness dependence of the Rashba SOI as a function of the gate bias voltage in InP/$In_{0.8}Ga_{0.2}As$/$In_{0.52}Al_{0.48}As$ asymmetric QWs.

The inverted–high electron mobility transistor (i-HEMT) structures with 5 and 10 nm QWs were grown on Fe-doped semi-insulating (100) InP substrate. The calculated band structure is shown in Figs. 1(a) and 1(b). It consists of, from the top, a 26.5 nm i-$In_{0.52}Al_{0.48}As$ cap layer, 5 nm (for 5 nm QW) or 2.5 nm (for 10 nm QW) i-InP layer, 5 or 10 nm i-$In_{0.8}Ga_{0.2}As$ QW, a 6 nm i-$In_{0.52}Al_{0.48}As$ spacer, a 6 nm *n*-$In_{0.52}Al_{0.48}As$ with Si density of $4\times10^{18}$ $cm^{-3}$, and a 200 nm i-$In_{0.52}Al_{0.48}As$ buffer layer. The epitaxial wafers were processed into $20\times80$ $\mu m^2$ Hall bars with 100-nm-thick $SiO_2$/Au front gate by standard photolithography and lift-off techniques. Applied external magnetic fields were perpendicular to the QW plane and magnetoconductance was measured with various gate bias voltages $V_g$ for analyzing the weak localization (WL) and the weak antilocalization (WAL) at $T=3.8$ K.

We first measured gate bias dependence of the sheet carrier density $N_s$ and the mobility $\mu$ at 3.8 K. Both $N_s$ and $\mu$ systematically change with the gate bias in 5 and 10 nm QWs and show linear increase as a function of the measured $V_g$. The $N_s$ is modulated from $1.18\times10^{12}$ to $2.54\times10^{12}$ $cm^{-2}$ in 5 nm QW and from $0.83\times10^{12}$ to $1.95\times10^{12}$ $cm^{-2}$ in 10 nm QW, respectively. Then, we measured magnetoconductance with various gate bias voltages in two different QWs, as shown in Fig. 2. For 5 nm QW, with increasing $V_g$ from $-4.3$ to $+2.5$ V, the positive magnetoconductance near zero magnetic field changes to the negative magnetoconductance where the clear crossover from the WL to the WAL is observed in the identical sample. It indicates that the strength of the Rashba SOI systematically changes from small to large with increasing $V_g$. On the other hand, for 10 nm QW, the WAL becomes dominant contribution at $V_g=-2.5$ V, and the WL is enhanced with increasing $V_g$, which suggest that the Rashba SOI weakens with applying the gate bias. To extract the Rashba SOI parameter $\alpha$, we fitted the experimental data by the quantum correction of the magnetotransport developed by Golub[30] in which we can apply the theory to ballistic and wider magnetic field range. Here we considered that the dominant SOI comes only from the SIA. It should be noted that SOI strengths derived by Iordanskii–Lyanda-Geller–Pikus (ILP) (Ref. 31) are very similar to those deduced from the Golub theory. The fitted data are shown with the solid lines in Figs. 2(a) and 2(b). The experimental data show clear deviations from the Golub theory at higher magnetic field regions. The reason for the deviations is thought to be due to the Dresselhaus SOI effect. The Golub theory can include either the Rashba SOI or the Dresselhaus SOI. When the Rashba SOI is weaker, the Dresselhaus SOI is not negligible. Actually the deviations are larger when the WAL effect is weaker as shown both in Figs. 2(a) and 2(b). The extracted $|\alpha|$ is plotted as a function of $N_s$ in Fig. 3. With increasing $N_s$, i.e., the gate bias voltage, the $|\alpha|$ of the 5 nm QW is found to increase, while that of 10 nm QW decreases. It reveals that two different QW thicknesses yield inverse $N_s$ dependence of the $|\alpha|$ in the same i-HEMT structures, where the energy band profile holds the same potential gradient. The gate controllability $d|\alpha|/dN_s$ is about $+2.0\times10^{-28}$ and $-3.0\times10^{-28}$ eV $m^3$ in 5 and 10 nm QWs, respectively. It suggests that the 10 nm QW enables the sensitive control of the Rashba SOI parameter and expects the larger transconductance for the application of the spin FET.[12] To understand the $N_s$ dependence of the obtained $|\alpha|$ in terms of the interface and the field contributions of the Rashba SOI, we calculated each components, $\alpha_{\text{interface}}$ and $\alpha_{\text{field}}$, of

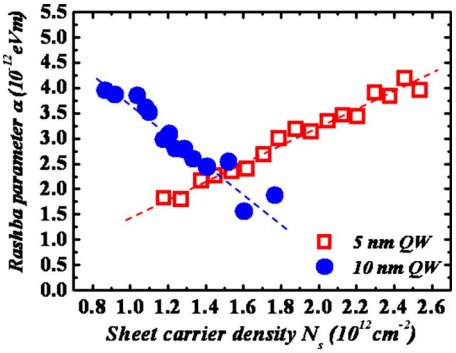


FIG. 3. (Color online) Sheet carrier dependence of the extracted Rashba SOI parameter $|\alpha|$ by the Golub theory. Open and closed circles show the results of 5 and 10 nm QWs, respectively.

the Rashba SOI parameter $\alpha_{\text{total}}$ from the $\boldsymbol{k}\cdot\boldsymbol{p}$ formalism.[11] We found that the calculated $\alpha_{\text{total}}$ also shows inverse $N_s$ dependences with the opposite sign in 5 and 10 nm QWs, where the experimental variations show a good agreement with the calculated $\alpha_{\text{total}}$ by changing the sign in 10 nm QW. It should be noted that we cannot determine the sign of the Rashba SOI parameter from the analysis of the magnetoconductance data.

For the 5 nm QW, large $\alpha_{\text{interface}}$ is induced since the electron probability density at the $In_{0.8}Ga_{0.2}As/InP$ interface becomes enhanced due to the strong confinement of the electrons inside the QW, while the negative $\alpha_{\text{field}}$ monotonically decreases with $N_s$ due to the suppression of the band bending by applying the gate bias. Consequently, positive $\alpha_{\text{total}}$ increases with the combination of $\alpha_{\text{interface}}$ and $\alpha_{\text{field}}$. On the other hand, in the case of 10 nm QW, $\alpha_{\text{interface}}$ is strongly suppressed due to the reduction in the electron probability density at the $In_{0.8}Ga_{0.2}As/InP$ interface, which resulted in the dominant contribution for $\alpha_{\text{total}}$ becoming negative slope of $\alpha_{\text{field}}$. A 5 nm difference in the QW thickness yields significant change in the gate bias dependence of $\alpha$. In turn, these results suggest that the QW thickness becomes crucial parameter for precise control of the Rashba SOI.

Gate controlled SOI, which gives rise to an effective magnetic field, provides an electrical way to manipulate spins. On the other hand, a momentum-dependent effective magnetic field due to the SOI randomizes spin orientations after several momentum scattering events. This is the so-called D'yakonov–Perel'[32] spin relaxation mechanism. The SOI is a double-edged sword because it can be used for spin manipulation; however, at the same time it causes spin relaxation. Therefore, it is very crucial to suppress the spin relaxation while keeping the strength and the controllability of SOI. Recently, several studies focusing on suppression of spin relaxation in the presence of SOI have been reported.[33–35] One of the ways to suppress spin relaxation is to confine electrons to moving one-dimensionally by narrow wire structures whose width is of same scale as bulk spin diffusion length $L_{\text{SO}}$ due to Rashba SOI. This suppression of spin relaxation due to lateral confinement effect has been theoretically investigated[33–35] and have been experimentally demonstrated through an optical way[21] and WAL analysis.[20]

Heterostructure used for narrow wire magnetotransport is an $InP/In_{0.53}Ga_{0.47}As$ (2.5 nm)/$In_{0.7}Ga_{0.3}As$ (10 nm)/$In_{0.53}Ga_{0.47}As$ (2.5 nm)/$In_{0.52}Al_{0.48}As$ layer structure epitaxially grown on (001) InP substrate. Sets of wires with gate electrode were fabricated using electron beam lithography and reactive ion etching as shown as an inset of Fig. 4(a). A set of wire consists of 95 identical wires with 650 $\mu$m long to suppress the universal conductance fluctuation (UCF). Geometrical width $W_{\text{SEM}}$ of wire defined by scanning electron microscopy (SEM) are 477, 566, 766, 861, 1026, and 1263 nm. Processed samples were covered with 150 nm thick of AuGeNi gate electrode isolated by 150 nm of $SiO_2$ gate insulator layer. To estimate transport properties of our sample, magnetoconductance measurement was performed on all sets of wires as well as Hall bar with the magnetic field range from 0 to 8 T at 0.3 K. To deduce the Rashba parameter $\alpha$ in the 2DEG, we fitted the ILP model to

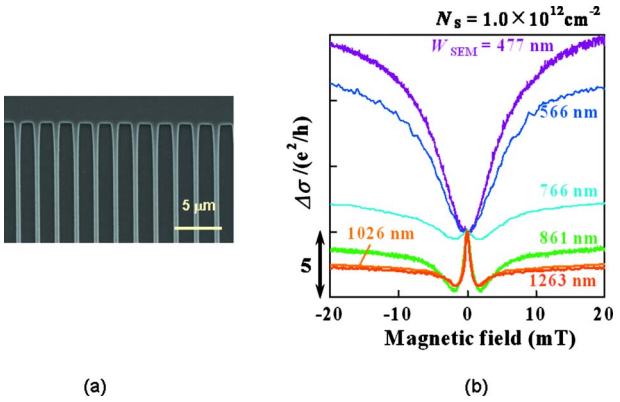


FIG. 4. (Color online) (a) A SEM picture of fabricated wire structure made of InGaAs QW. (b) Width dependence of magnetoconductance data.

WAL observed in a Hall bar and extracts the Rashba parameter of $\alpha=3.0\times10^{-12}$ eV m at $N_s=1.0\times10^{12}$ cm$^{-2}$ and corresponding bulk spin diffusion length of $L_{\text{SO}}=\hbar^2/2\alpha m^*=0.3$ $\mu$m.

We now turn to the investigation of transport properties in narrow wire structures. Conductance of narrow wire structures at the zero external magnetic field shows a linear width dependence. The depletion width $W_{\text{dep}}=309$ nm due to surface energy pinning is deduced from the $x$-intercept of the linear dependence. The clear Shubnikov–de Haas (SDH) oscillation was observed in all samples. From fast Fourier transform of $1/B$ plots, carrier density $N_s$ and mobility $\mu$ are determined. $N_s$ and $\mu$ of narrow wires are almost constant on the wire width. It should be noted that the strength of the Rashba SOI is not changed by making wires narrow in this width range. We then carefully measured magnetoconductance in low magnetic field of $B=\pm30$ mT to discuss spin relaxation. Results of this measurement are shown in Fig. 4(b). Clear crossover from WAL to WL is observed with changing $W_{\text{SEM}}$ from 1263 to 477 nm. This $W_{\text{SEM}}$ dependence of magnetoconductance indicates that lateral confinement effect obviously exists in our samples. Since wires of $W_{\text{SEM}}=1026$ and 1263 nm show quite similar curves in Fig. 4(b), lateral confinement effect starts when the width is less than $W_{\text{eff}}=W_{\text{SEM}}-W_{\text{dep}}=861-309=552$ nm, although wire effective width still exceeds bulk spin diffusion length. At $W_{\text{SEM}}=766$ nm, the conductance peak around $B=0$ due to spin relaxation is almost suppressed. The conductance peaks disappear at $W_{\text{SEM}}=566$ nm and 477 nm. This width dependence of the magnetoconductance clearly shows that the spin relaxation is suppressed by the lateral confinement. Furthermore, we have observed enhancement in spin relaxation time by making the Rashba SOI strength approach that of the Dresselhaus SOI by applying the gate voltage.[36] There are two ways to suppress the spin relaxation due to the SOI. Geometrical confinement is effective to suppress the spin relaxation when the width of wires is shortened in the order of bulk spin diffusion length. Another way is to make the Rashba SOI equal the Dresselhaus SOI. These methods work because the spin relaxation mechanism in our heterostructures is governed by D'yakonov–Perel' spin relaxation mechanism.[32] Recently, we have proposed a novel method to

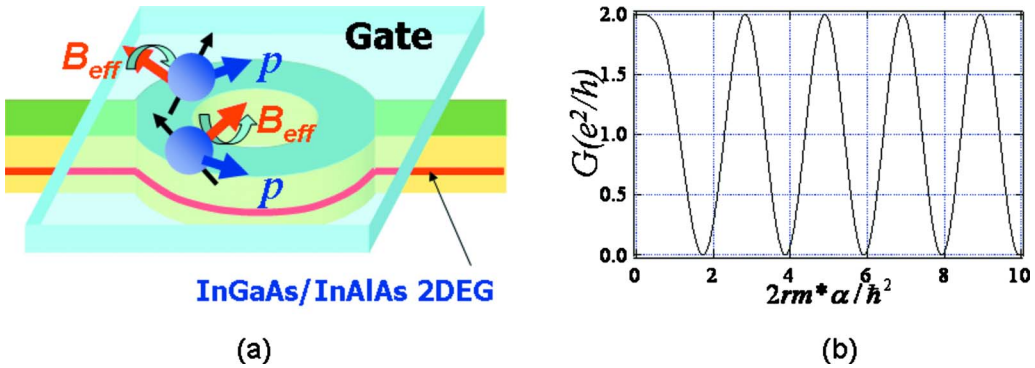


FIG. 5. (Color online) (a) Schematic structure of the proposed spin interference device. The Rashba SOI is tunable by a gate voltage. (b) The conductance of a one-dimensional ring as a function of the Rashba SOI strength $\alpha$.

detect the relative strength of Rashba and Dresselhaus SOIs in quantum wires by electrical measurement.[37]

## IV. SPIN INTERFEROMETER AND ELECTRONIC AC EFFECT

A rotation operator for spin 1/2 produces minus sign under $2\pi$ rotation.[38] Neutron spin interference experiments performed by two groups verified this extraordinary prediction of quantum mechanics.[2,3] In solids, an electron spin interference experiment in a *n*-GaAs interference loop has been conducted using optical pump and probe methods.[39] A local magnetic field due to dynamic nuclear spin polarization caused spin precession of the wave packet in one of the interference paths. In the above spin interference experiments, spin precession was controlled by a local magnetic field. To confirm the AC effect, we need to control spin rotation by an electric field. Mathur and Stone[24] theoretically showed that the effects of SOI in disordered conductors are manifestations of the AC effect in the same sense as the effects of weak magnetic fields are manifestations of AB effect. Qian and Su[40] obtained the AC phase, which is the sum of spin-orbit Berry phase and spin dynamical phase in a one-dimensional ring with SOI.

In the presence of an external magnetic field and an electric field, the one-particle Hamiltonian can be expressed as[26]

$$H = \frac{(\vec{p} - e\vec{A} - \mu_B \vec{\sigma} \times \vec{E}/2c^2)^2}{2m_0}. \tag{5}$$

The contribution from the vector potential $\vec{A}$ corresponds to the AB phase and the contribution from the SOI to the AC phase. In this paper, we assume that the Rashba SOI is stronger than the Dresselhaus SOI,[25] and we only take the Rashba SOI into account. We have proposed a spin interference device based on the Rashba SOI as shown in Fig. 5(a).[41] The AC phases acquired by the spin wave functions during a cyclic evolution are calculated in a mesoscopic ring in the presence of the Rashba SOI.[41–43] The origin of the spin interference is the spin precession angle difference between the left and right branches. The phases acquired in the left and right branches are not the same; they have an opposite sign because the precession orientation is opposite. It is interesting that the obtained AC dynamical phase is very similar to that of the spin FET. The origin of the phase difference in both cases is related to the spin precession. By using the spin interference device, we can investigate how much the spin precession angle can be controlled by a gate voltage. Furthermore, an observation of spin interference in a mesoscopic ring is an experimental demonstration of the electronic AC effect.

The total Hamiltonian of a one-dimensional ring with the Rashba SOI in cylindrical coordinates reads[44]

$$H(\phi) = \frac{\hbar^2}{2m^* r^2}\left(-i\frac{\partial}{\partial\phi} + \frac{\Phi}{\Phi_0}\right)^2 + \frac{\alpha}{r}(\cos\phi\sigma_x + \sin\phi\sigma_y) \times \left(-i\frac{\partial}{\partial\phi} + \frac{\Phi}{\Phi_0}\right) - i\frac{\alpha}{2r}(\cos\phi\sigma_y - \sin\phi\sigma_x) + \frac{\hbar\omega_B}{2}\sigma_z. \tag{6}$$

Here an external magnetic field $B_z$ is applied in the *z*-direction, which is perpendicular to the ring plane, and magnetic flux through the ring is given by $\Phi = B_z \pi r^2$, with ring radius *r*; $\Phi_0 = h/e$ is the flux quantum. The polar angle is given by $\phi$. $\omega_B = 2\mu_B B_z/\hbar$ is the Larmor frequency. In an isolated ring, the wave function is given by the following form:

$$\Psi = \frac{1}{\sqrt{2\pi}}\begin{pmatrix} C_n^+ e^{in\phi} \\ C_n^- e^{in\phi} \end{pmatrix}, \tag{7}$$

where $C_n^+$ and $C_n^-$ are coefficients of spin-up and spin-down eigenstates, respectively. When the Zeeman term is negligible, the energy eigenvalues can be written as[26]

$$E_{n,s} = \hbar\omega_0\left[n + \frac{\Phi}{\Phi_0} - \frac{\Phi_{\mathrm{AC}}^s}{2\pi}\right]^2, \tag{8}$$

with $\omega_0 = \hbar/2m^* r^2$, *n* integer, and the AC phase $\Phi_{\mathrm{AC}}^s$. The AC phase is given by[26,41–43,45]

$$\Phi_{\mathrm{AC}}^s = -\pi\left[1 + s\sqrt{\left(\frac{2rm^*\alpha}{\hbar^2}\right)^2 + 1}\right], \quad s = \pm. \tag{9}$$

This AC phase can be viewed as an effective spin dependent magnetic flux through the ring, which modulates the conductance of the ring. Here $s = \pm$ corresponds to spin-up and spin-down along the effective magnetic field. From the above calculation, the conductance when electrons travel halfway

around the ring at $B_z=0$ is written as[26,41–43,45]

$$G = \frac{e^2}{h}\left[1 - \cos\left\{\pi\sqrt{1+\left(\frac{2rm^*\alpha}{\hbar^2}\right)^2}\right\}\right]. \quad (10)$$

This equation shows that the conductance of the ring oscillates as a function of the strength $\alpha$ of Rashba SOI as shown in Fig. 5(b). This SOI dependence is very similar to the conductance of the spin FET proposed by Datta and Das[12] in which they need ferromagnetic electrodes for spin injection and detection. This proposed spin interferometer works without ferromagnetic electrodes.

## V. AC SPIN INTERFERENCE EXPERIMENT

The resistance of a mesoscopic ring is affected by several quantum interference effects. The well known AB effect results in a resistance oscillation with a magnetic flux period of $h/e$. The AB effect is sample specific and very sensitive to the Fermi wavelength; therefore, the interference pattern is rapidly changed by the gate voltage. In order to detect the AC effect we used another quantum interference phenomenon, the AAS effect.[28,46] The AAS effect is an AB effect of time reversal symmetric paths, where the two wave function parts go all around back to the origin on identical paths but in opposite directions. In this situation any phase that is due to path geometry will be identical and will not affect the interference. This also means that it is independent of the Fermi energy $E_F$ (and consequently the carrier density $N_s$). However, the AAS effect is sensitive to the spin phase when the SOI plays a role. If there is magnetic flux inside the paths the resistance will oscillate with the period of $h/2e$. When the flux is increased the resistance oscillates with the period $h/2e$, but the AAS oscillation amplitude decays after a few periods because of averaging between different paths in the ring with different areas. If there is SOI in the ring, the electron spin will start precessing around the effective magnetic field and change the interference at the entry point. Note that the effective magnetic field due to the SOI is much stronger than the external magnetic field to pick up AAS oscillations. The precession axes for the two parts of the wave function are opposite, and therefore the relative precession angle is twice the angle of each part. If the relative precession angle is $\pi$ the spins of the two parts are opposite and cannot interfere, and the AAS oscillations disappear. If the relative angle is $2\pi$ the two parts will have the same spin but opposite signs because of the 1/2 spin quantum laws (a $4\pi$ rotation is required to return to the original wave function), effectively changing the phase of the AAS oscillations by $\pi$, which we interpret as a negative amplitude.

By using arrays rather than single rings we get a stronger spin signal, and we average out some of the UCFs and sample specific AB oscillations.[46] Complex gate voltage dependence has been reported in an AB-type AC experiment in a single ring fabricated from HgTe/HgCdTe QWs.[47] Therefore, a detailed analysis is necessary to compare with AC theory. A spin geometrical phase effect has been studied in a single AB ring using a *p*-type GaAs heterostructure.[48]

The ring arrays were etched out in an electron cyclotron resonance dry-etching process from an InP/InGaAs/InAlAs based 2DEG, the same as used for the SDH measurements. The electron mobility was 7–11 $m^2/V\,s$ depending on the carrier density, and the effective electron mass $m^*$ was $0.050m_0$ as determined from the temperature dependence of SDH oscillation amplitudes. Figure 6 shows an example of the ring array, which consists of $4\times4$ rings of 1.0 $\mu$m radius. Note that the actually measured sample was a $5\times5$ ring array. The rings were covered with a 50 nm thick $SiO_2$ insulator layer and an Au gate electrode, used to control the carrier density and the SOI parameter $\alpha$. In the present sample, we design the array with a small number of rings in order to escape a gate tunneling leakage problem. The advantage of using a small number of rings rather than a large array is that the gate tunneling leakage is much smaller and we can use a relatively high gate voltage.[27] This makes it possible to see several oscillations of AC interference. Earlier experiments on square loop arrays with very large number of loops showed convincing spin interference results but only up to one interference period.[49,50]

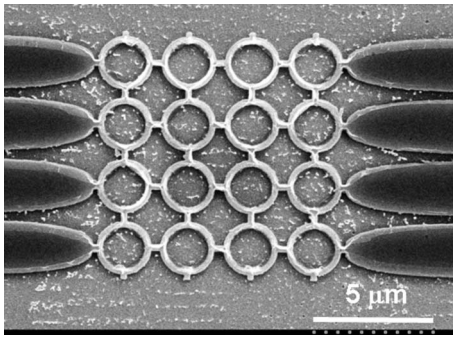


FIG. 6. A SEM image of an array of rings with 1 $\mu$m radius using an InGaAs/InAlAs heterostructure.

The experiment was carried out in a $^3$He cryostat at the base temperature, which varied between 220 and 270 mK. The sample was put in the core of a superconducting magnet with the field $B$ perpendicular to the 2DEG plane. We measured the resistance $R$ of the ring array simultaneously with the Hall resistance $R_H$ of the Hall bar close to the rings while stepping the magnetic field and the gate voltage $V_g$. Close to the arrays and in the same current path and under the same gate was a Hall bar 5 $\mu$m wide and 20 $\mu$m long that is used to measure the carrier density. We calculated the carrier density $N_s$ from the slope of the $R_H$ versus $B$ ($N_s^{-1}=edR_H/dB$), and the carrier concentration is linearly increased with the gate voltage $V_g$.

In order to reduce noise and UCF effects we averaged ten resistance versus magnetic field ($R$ versus $B$) curves with slightly different gate voltages. This averaging preserves the AAS oscillations, but the averaging of $M$ curves reduces the AB amplitude roughly as $M^{-1/2}$. We took the FFT spectrum (using an Exact Blackman window) of this average and got a spectrum with two peaks, corresponding to the AB oscillations and the AAS oscillations at twice the frequency. We integrated the area of the AAS peak to get the amplitude and determined the sign by analyzing the phase of the central part of the filtered $R$ versus $B$ data.

In Fig. 7, we display the $h/2e$ magnetoresistance oscillations due to the AAS effect at five different gate voltages.

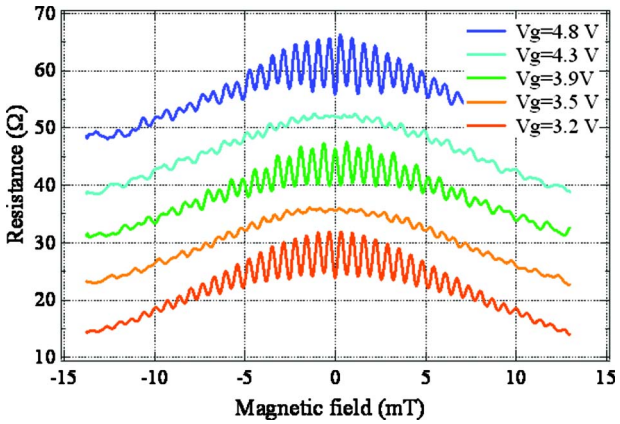


FIG. 7. (Color online) Magnetoresistance oscillations with period of $h/2e$ due to the AAS effect at five different gate voltages. The curves are shifted vertically for clarity. The oscillations in the top and bottom curves are reversed compared to the middle one because of the AC effect. The oscillation amplitudes for second and fourth curves are suppressed. These gate voltage dependent AAS oscillations are due to the AC effect.

The oscillations in the top and bottom curves are reversed compared to the middle one because of the AC effect. The second and fourth curves have almost no oscillations; the spin precession rotates the spins of the two wave function parts to opposite directions. Figure 8 shows the color scale plot after digital band-pass filtering of the AAS oscillations, which are visible as vertical stripes in the figure. We can clearly see the oscillations switching phase as we increase the gate voltage. We then plotted the amplitude against the gate voltage as shown in Fig. 9. The AAS amplitude oscillates as a function of the gate voltage, which changes the SOI parameter $\alpha$. As we discuss below using Eqs. (11) and (12) the amplitude crosses zero, inverting the AAS oscillations. Each period represents one extra $2\pi$ spin precession of an electron moving around a ring.

In the FFT spectra there is also a small peak at $h/4e$. This is due to the wave function parts going twice around the ring before interfering. If we do the same analysis on this peak we get an oscillating amplitude with half the period compared to the $h/2e$ amplitude. This is expected because the distance is twice, and therefore the precession angle is also twice. Both $h/2e$ and $h/4e$ oscillation amplitudes increase with increasing the gate voltage $V_g$. This is because the spin coherence length of ring becomes longer with increasing diffusion constant, which depends on the carrier density. The spin coherence length is estimated to be 3.4 $\mu$m from the ratio between $h/2e$ and $h/4e$ oscillation amplitudes. This value is not long if we consider that the channel width is less than 0.2 $\mu$m, where the long spin relaxation length is expected. In this AC interference experiment, the interference is cut off not by spin relaxation length but by inelastic scattering length. Actually we have observed sudden suppression of AC interference amplitude when the channel of the rings is occupied by the second subband where inelastic scattering due to the inter subband scattering takes place.[51] It should be noted that the spin relaxation length is more important than the inelastic scattering length in noninterference devices such as the spin FET.

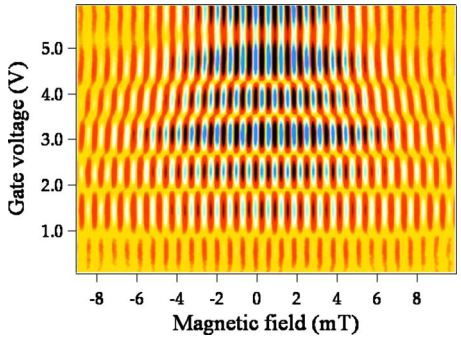


FIG. 8. (Color online) The $h/2e$ oscillations are plotted against the gate voltage. The oscillations reverse phase at several gate voltages due to the AC effect (Ref. 27).

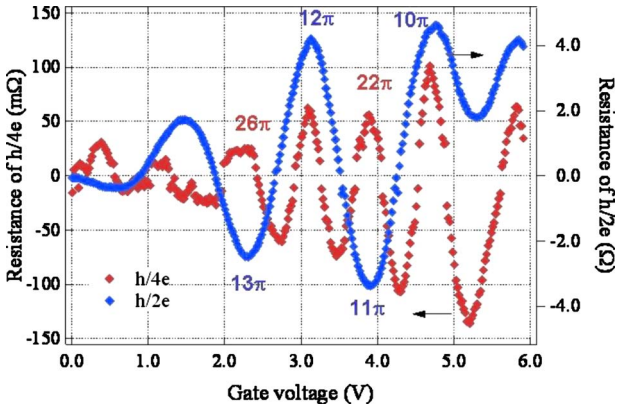


FIG. 9. (Color online) AC oscillations of the first and second harmonics. The second harmonic corresponds to two turns around the ring before interfering. The period of the second harmonic is half the first harmonic period as expected (Ref. 27).

The precession angle $\theta$ of an electron moving along a straight narrow channel is given by[12]

$$\theta = \frac{2\alpha m^*}{\hbar^2} L, \tag{11}$$

with $L$ being the travel distance. The modulation of the $h/2e$ oscillation amplitude can be expressed as a function of $\alpha$,

$$\frac{\delta R_\alpha}{\delta R_{\alpha=0}} = \cos\left\{2\pi\sqrt{1+\left(\frac{2m^*\alpha}{\hbar^2}r\right)^2}\right\}, \tag{12}$$

where $\delta R_\alpha$ and $\delta R_{\alpha=0}$ is the $h/2e$ amplitude with and without SOI, respectively. In relating the result of the spin interference experiment to the spin precession angle, the argument of cosine in Eq. (12) reduces to the spin precession angle $\theta$ in the limit of strong SOI or large ring radius because the distance traveled around the ring is $2\pi r$.

We also measured SDH oscillations at different carrier densities in a separate Hall bar. The SOI strength $\alpha$ obtained from the beating pattern of the SDH oscillations shows carrier density dependence because the Rashba SOI depends on the SIA and therefore on the shape of the QW, which is modified by applying the gate voltage. The gate voltage sensitivity $\Delta\alpha/\Delta V_G$ is about $0.51\times10^{-12}$ eV m/V in the present heterostructure. From the gate voltage dependence of SOI $\alpha$ we estimate the spin precession angles at several different gate voltages. The estimated spin precession angles at the peak and dips of the AC oscillations are shown in Fig. 9.

It is found that the spin precession angle is controlled over the range of $4\pi$ by the gate electric field. We could observe more than $20\pi$ spin precession angle.

This clear demonstration of the AC interference controlled by the gate electric field can be attributed to the fact that the SOI is much enhanced in semiconductor heterostructures compared to the SOI in vacuum. The AC effect is of fundamental importance for quantum interference phenomena and quantum interactions.

## VI. CONCLUSION

We discuss the enhancement in SOI and the origin of Rashba SOI. QW thickness dependence of the Rashba SOI strength is investigated in InP/InGaAs/InAlAs asymmetric QWs by analyzing WAL. Two different QW thicknesses show inverse $N_s$ dependence of the Rashba SOI strength in the same heterostructures. We confirm that narrow wires are effective to suppress spin relaxation. It is shown that a spin interferometer based on the Rashba SOI is equivalent to an electronic AC interference experiment. The conductance oscillation of the spin interferometer as a function of the Rashba SOI is very similar to the Datta–Das spin FET, but ferromagnetic source and drain electrodes are not necessary in the spin interferometer. We have demonstrated the electronic AC effect dual to the magnetic AAS effect in small arrays of rings. The AC interference oscillations are controlled over several periods. This result shows that the spin precession rate can be controlled in a precise and predictable way by an electrostatic gate. The electrical manipulation of spins and suppression of spin relaxation in narrow wires are of crucial importance in order to realize semiconductor spintronics devices based on SOI.

The authors thank J. Ohe, T. Ohtsuki, T. Koga, Y. Sekine, T. Kobayashi, F. Meijer, M. van Veenhuizen, T. Nihei, and J. Takagi for their valuable discussions. This work is partly supported by Grant-in-Aids from JSPS and MEXT. J.N. acknowledges the Mitsubishi Foundation.

[1]W. Gerlach and O. Stern, Z. Phys. **9**, 349 (1922).
[2]H. Rauch, A. Zeilinger, G. Badurek, A. Wilfing, W. Bauspiess, and U. Bonse, Phys. Lett. A **54**, 425 (1975).
[3]S. A. Werner, R. Colella, A. W. Overhauser, and C. F. Eagen, Phys. Rev. Lett. **35**, 1053 (1975).
[4]E. I. Rashba, Sov. Phys. Solid State **2**, 1109 (1960); Y. A. Bychkov and E. I. Rashba, J. Phys. C **17**, 6039 (1984).
[5]S. A. Wolf, D. D. Awschalom, R. A. Buhrman, J. M. Daughton, S. Von Molnar, M. L. Roukes, A. Y. Chtchelkanova, and D. M. Treger, Science **294**, 1488 (2001).
[6]D. D. Awschalom, N. Samarth, and D. Loss, *Semiconductor Spintronics and Quantum Computation* (Springer, Heidelberg, 2002).
[7]I. Zutic, J. Fabian, and S. Das Sarma, Rev. Mod. Phys. **76**, 323 (2004).
[8]D. D. Awschalom and M. E. Flatte, Nat. Phys. **3**, 153 (2007).
[9]J. Nitta, T. Akazaki, H. Takayanagi, and T. Enoki, Phys. Rev. Lett. **78**, 1335 (1997); T. Koga, J. Nitta, T. Akazaki, and H. Takayanagi, *ibid.* **89**, 046801 (2002).
[10]G. Engels, J. Lange, Th. Schäpers, and H. Lüth, Phys. Rev. B **55**, R1958 (1997).
[11]Th. Schäpers, G. Engels, J. Lamge, Th. Klocke, M. Hollfelder, and H. Lüth, J. Appl. Phys. **83**, 4324 (1998).
[12]S. Datta and B. Das, Appl. Phys. Lett. **56**, 665 (1990).
[13]J. Ohe, M. Yamamoto, T. Ohtsuki, and J. Nitta, Phys. Rev. B **72**, 041308(R) (2005).
[14]M. I. Dyakonov and V. I. Perel', Phys. Lett. A **35**, 459 (1971).
[15]J. E. Hirsch, Phys. Rev. Lett. **83**, 1834 (1999).
[16]S. Murakami, N. Nagaosa, and S. C. Zhang, Science **301**, 1348 (2003).
[17]J. Sinova, D. Culcer, Q. Niu, N. A. Sinitsyn, T. Jungwirth, and A. H. MacDonald, Phys. Rev. Lett. **92**, 126603 (2004).
[18]Y. K. Kato, R. C. Myers, A. C. Gossard, and D. D. Awschalom, Science **306**, 1910 (2004).
[19]J. Wunderlich, B. Kaestner, J. Sinova, and T. Jungwirth, Phys. Rev. Lett. **94**, 047204 (2005).
[20]Th. Schäpers, V. A. Guzenko, M. G. Pala, U. Zülich, M. Governale, J. Knobbe, and H. Hardtdegen, Phys. Rev. B **74**, 081301(R) (2006).
[21]A. W. Holleitner, V. Sih, R. C. Myers, A. C. Gossard, and D. D. Awschalom, Phys. Rev. Lett. **97**, 036805 (2006).
[22]Y. Aharonov and A. Casher, Phys. Rev. Lett. **53**, 319 (1984).
[23]A. Cimmino, G. I. Opat, A. G. Klein, H. Kaiser, S. A. Werner, M. Arif, and R. Clothier, Phys. Rev. Lett. **63**, 380 (1989).
[24]H. Mathur and A. D. Stone, Phys. Rev. Lett. **68**, 2964 (1992).
[25]G. Dresselhaus, Phys. Rev. **100**, 580 (1955).
[26]X. F. Wang and P. Vasilopoulos, Phys. Rev. B **72**, 165336 (2005).
[27]T. Bergsten, T. Kobayashi, Y. Sekine, and J. Nitta, Phys. Rev. Lett. **97**, 196803 (2006).
[28]B. L. Al'tshuler, A. G. Aronov, and B. Z. Spivak, JETP Lett. **33**, 94 (1981).
[29]R. Winkler, *Spin-Orbit Coupling Effects in Two-Dimensional Electron and Hole Systems*, Springer Tracts in Modern Physics Vol. 191 (Springer-Verlag, Berlin, 2003).
[30]L. E. Golub, Phys. Rev. B **71**, 235310 (2005).
[31]S. V. Iordanskii, Y. B. Lyanda-Geller, and G. E. Pikus, JETP Lett. **60**, 206 (1994).
[32]M. I. D'yakonov and V. I. Perel', Sov. Phys. Solid State **13**, 3023 (1971).
[33]A. G. Mal'shukov and K. A. Chao, Phys. Rev. B **61**, R2413 (2000).
[34]A. A. Kiselev and K. W. Kim, Phys. Rev. B **61**, 13115 (2000).
[35]S. Kettemann, Phys. Rev. Lett. **98**, 176808 (2007).
[36]Y. Kunihashi, M. Kohda, and J. Nitta (unpublished).
[37]M. Scheid, M. Kohda, Y. Kunihashi, K. Richter, and J. Nitta, Phys. Rev. Lett. **101**, 266401 (2008).
[38]J. J. Sakurai, *Modern Quantum Mechanics* (Benjamin/Cummings, Menlo Park, CA, 1985).
[39]Y. K. Kato, R. C. Myer, A. C. Gossard, and D. D. Awschalom, Appl. Phys. Lett. **86**, 162107 (2005).
[40]T.-Z. Qian and Z.-B. Su, Phys. Rev. Lett. **72**, 2311 (1994).
[41]J. Nitta, F. E. Meijer, and H. Takayanagi, Appl. Phys. Lett. **75**, 695 (1999).
[42]D. Frustaglia and K. Richter, Phys. Rev. B **69**, 235310 (2004).
[43]S.-Q. Shen, Z.-J. Li, and Z. Ma, Appl. Phys. Lett. **84**, 996 (2004).
[44]F. E. Meijer, A. F. Morpurgo, and T. M. Klapwijk, Phys. Rev. B **66**, 033107 (2002).
[45]M. J. van Veenhuizen, T. Koga, and J. Nitta, Phys. Rev. B **73**, 235315 (2006).
[46]C. P. Umbach, C. Van Haesendonck, R. B. Laibowitz, S. Washburn, and R. A. Webb, Phys. Rev. Lett. **56**, 386 (1986).
[47]M. König, A. Tschetschetkin, E. M. Hankiewiccz, J. Sinova, V. Hock, V. Daumer, M. Schaefer, C. R. Becker, H. Buhmann, and L. W. Molenkamp, Phys. Rev. Lett. **96**, 076804 (2006).
[48]B. Grbic, R. Leturcq, Th. Ihn, K. Ensslin, D. Reuter, and A. D. Wieck, Phys. Rev. Lett. **99**, 176803 (2007).
[49]T. Koga, J. Nitta, and M. van Veenhuizen, Phys. Rev. B **70**, 161302(R) (2004).
[50]T. Koga, Y. Sekine, and J. Nitta, Phys. Rev. B **74**, 041302(R) (2006).
[51]J. Takagi, M. Kohda, and J. Nitta (unpublished).